Articles   School of Civil and Structural Engineering

2015

Nonlinear Analysis of Isotropic Slab Bridges under Extreme Traffic Loading

Donya Hajializadeh
University College Dublin

A. Salam Al-Sabah
University College Dublin

Eugene J. OBrien
University College Dublin

Debra F. Laefer
University College Dublin

Bernard Enright
Technological University Dublin, bernard.enright@tudublin.ie

Follow this and additional works at: https://arrow.tudublin.ie/engschcivart

Part of the Civil Engineering Commons, and the Structural Engineering Commons

Recommended Citation

Nonlinear Analysis of Isotropic Slab Bridges under Extreme Traffic Loading

Donya Hajializadeh[1], A. Salam Al-Sabah[2], Eugene J. OBrien[1,2], Debra F. Laefer[2], Bernard Enright[3]

[1]Roughan & O'Donovan Innovative Solutions, Ireland

[2]University College Dublin, Ireland

[3]Dublin Institute of Technology, Ireland

Abstract

Probabilistic analysis of traffic loading on a bridge traditionally involves an extrapolation from measured or simulated load effects to a characteristic maximum value. In recent years, Long Run Simulation, whereby thousands of years of traffic are simulated, has allowed researchers to gain new insights into the nature of the traffic scenarios that govern at the limit state. For example, mobile cranes and low-loaders, sometimes accompanied by a common articulated truck, have been shown to govern in most cases. In this paper, the extreme loading scenarios identified in the Long Run Simulation are applied to a non-linear, two-dimensional (2D) plate finite element model. For the first time, the loading scenarios that govern in 2D nonlinear analyses are found and compared to those that govern for 2D linear and 1D linear/nonlinear analyses. Results show that, for an isotropic slab, the governing loading scenarios are similar to those that govern in simple one-dimensional (beam) models. Furthermore, there are only slight differences in the critical positions of the vehicles. It is also evident that the load effects causing failure in the 2D linear elastic plate models are significantly lower, i.e. 2D linear elastic analysis is more conservative than both 2D nonlinear and 1D linear/nonlinear.

1.1 Introduction

A key part of bridge management is the assessment of the safety of bridge structures. A bridge is considered to be safe when its capacity to resist load exceeds the effect of the load applied. Substantial work has been conducted to develop methods of evaluating the load-carrying capacity of bridges and the associated uncertainties. In comparison, traffic loading on bridges has received less attention. The load models used to represent traffic in safety assessment analysis are often over-simplified or taken from conservative standards or codes. Site-specific, bridge assessment based on realistic load models offers the potential of significant cost savings in maintenance budgets (O'Connor and Enevoldsen 2009).

In recent years, improvement in the availability and quality of Weigh-In-Motion (WIM) data has facilitated this. While WIM data are becoming more widely available, the quantity of traffic data is generally not sufficient to cover the return periods of interest. One approach to extend measured traffic data is to use statistical information from measurements to find the best-fit distributions to load effects and to use these distributions as a basis for extrapolation to find the characteristic lifetime, maximum values (Nowak 1993; Miao and Chan 2002). However, there is significant uncertainty both in the estimated characteristic load effects (Dawe 2003; Gindy and Nassif 2006) and in the critical loading scenarios. An alternative approach is to use Monte Carlo simulations on synthetically generated traffic data that has been calibrated against measured traffic characteristics, such as vehicle weights, in-lane gaps, and inter-lane gaps (Bailey and Bez 1999; O'Connor and OBrien 2005). Notably, even short run simulations of this type still require some form of statistical extrapolation based on the load effect history, and to avoid the uncertainty resulting from this extrapolation, it is necessary to run the simulation for an extended time period. Enright (2010) and Enright and OBrien (2012) develop a carefully optimized Monte Carlo simulation program to simulate traffic for thousands of years. While it is still an extrapolation, this reduces the variability associated with the fitting to statistical distributions by modelling the rare traffic events in traffic directly. These 'long-run' simulations provide examples of extreme loading scenarios, thereby illustrating the types and combinations of vehicles expected to feature in extreme bridge loading events. Enright's simulations are calibrated against extensive WIM data collected from five European countries: the Netherlands, Slovakia, the Czech Republic, Slovenia, and Poland. Long-run simulation is used in this paper, as it is the only approach that provides sufficient information to run a nonlinear analysis of the critical scenarios.

In earlier work (Hajializadeh at al. 2012), the authors focused on 1D nonlinear analysis of two-span bridges subject to extreme traffic loads. In this study two-dimensional (2D), nonlinear analysis is performed on simply-supported, solid, isotropic bridges of varying lengths and depths. The bridges are subjected to characteristic loading scenarios resulting from long-run simulations for three European sites: the Netherlands, Slovakia, and the Czech Republic. For each case, a load ratio is calculated (i.e., the factor that the loading needs to be multiplied by to cause failure). The load ratio for the 2D nonlinear analysis is compared to the factor calculated using a one-dimensional (1D) and 2D linear analyses.

The nonlinear nature of reinforced concrete causes the redistribution of bending moments when a structure is subjected to a load beyond the service load range. The assumption of linear behavior is accurate for low stress levels, but as ultimate capacity at critical sections is approached, the load is transferred to other parts of the structure. Allowing for this extra reserve of strength in a redundant structure results in a more economical bridge assessment. The research conducted in this study, can be applied to all existing solid slab bridges in order to verify the structural safety at the ultimate limit state and could also be applied to new bridges. It should be noted that vehicle/bridge dynamic interaction is not considered – the analysis is just static.

1.1.1 Yield Line Analysis

Yield line analysis starts by assuming a yield collapse pattern and then obtaining the collapse load, usually through the application of virtual work. As the yield line is an upper bound method, the theoretical collapse load is the minimum of the collapse loads resulting from all kinematically admissible yield collapse patterns.

Yield line theory is first introduced by Ingerslev (1923). Ingerslev performs the analysis for a simply supported rectangular slab by considering the equilibrium between loads and bending moments at yield lines. Later, Johansen (1962) continues Ingerslev's (1923) work with a geometric interpretation of the concept. Through the work of Johansen (1962, 1972), Jones and Wood (1967) and Nielsen (1964), yield line analysis is today applied to a wide range of theoretical and practical applications.

An integrated form of yield line method is proposed by Munro and Da Fonseca (1978) that incorporates finite elements and linear programming. They use triangular finite elements, assuming that yield lines can only develop along element edges. This methodology identifies the critical yield pattern, (i.e., there is no need to identify initially the collapse mechanism). However, collapse mechanisms are limited to the available patterns defined by the applied triangular finite element mesh. Jennings et al. (1993) address the variation of mechanism geometry using a geometrical optimization technique in conjunction with the linear programming algorithm. Thavalingam et al. (1998) use an approach similar to that of Munro and Da Fonseca (1978) by developing a semi-automatic, yield line analysis where the initial yield pattern is represented by variable node positions.

A fixed finite element mesh requires an initial pattern to be defined based on the expected yield mechanism. Further attempts have been made to resolve this issue. Bauer and Redwood (1987) compute the yield load of a plate based on assumed collapse mechanisms generated by moving one or more of the nodes used initially in defining the yield line pattern. Dickens and Jones (1988) manually adjust the assumed trial yield pattern to reach a closer, overall ratio of plastic moment to collapse load for the entire slab in each rigid slab regionJohnson (1994) conducts a rigid-plastic yield line analysis of isotropic slabs under a uniformly distributed load, using a two-step procedure. In the first step, a yield pattern is predicted using a linear finite element analysis, then a less refined mesh is constructed with element boundaries lying close to the expected yield lines, to obtain the yield mechanism. Johnson (1996) extends the method developed for isotropic slabs (Johnson 1995) to non-isotropic cases.

Gohnert and Kemp (1995) propose a four-node element, which they termed a "yield line element". Gohnert (2000) uses this element in yield line analysis while assuming elastic-perfectly plastic behavior. Reported results are within 10% of previous published yield line analyses for the same examples (Johansen 1962).

Taking a different approach, Kwan (2004) proposes a method to resolve the difficulty of generating kinematically admissible yield line patterns by introducing 'dip' and 'strike' angles. These angles are used to define the orientation of the rotation axis (strike angle) and the amount of rotation (dip angle) of each region in the yielded slab. Although this method

generates accurate results, it is limited to convex polygonal slabs. To overcome this, Wüst and Wagner (2008) present a systematic approach in which all possible yield mechanisms of an arbitrary polygonal plate can be found. They use elements similar to those proposed by Munro and Da Fonseca (1978) to triangulate the resulting patterns.

Jackson and Middleton (2009) propose a new method using Johansen's yield surface. This is based on the lower bound theory of plasticity, equilibrium of the finite elements, and optimization is achieved by conic programming. This method predicts collapse mechanisms close to those found by Johansen's yield line analysis (Johansen 1962).

An alternative approach to yield line analysis is the lower-bound strip method proposed by Hillerborg (1975), in which the total load is assumed to be distributed between two sets of orthogonal strips. O'Dwyer and OBrien (1998) modify this strip method using linear and quadratic programming optimization. An automated lower-bound method is presented by Burgoyne and Smith (2008).

Generally nonlinear finite element analyses have been shown to model concrete material behavior more realistically than linear analyses. Such approaches have the additional ability to obtain more information about the slab responses such as deflection and reactions. Powerful commercial software packages which use nonlinear 2D methods are now available but are problematic, because of numerical instability due to the highly nonlinear nature of cracked concrete and the substantial time required to solve full-scale problems. To overcome these drawbacks a lower bound, yield line, finite element analysis approach has recently been developed, as described below, and this approach is adopted in this paper.

1.2 Finite Element Lower Bound "Yield Line" Analysis

Al-Sabah and Falter (2013) describe a method which can be used as a computationally-efficient alternative to currently available, nonlinear finite element software packages. The method is simple, widely applicable, quick, and economical. Specifically, they use modified, rotation-free, plate finite elements to allow plastic "yield lines" to pass through an element. Yield is progressively introduced to the elements with each additional load increment until failure is detected. This method is used here to account for the nonlinear post-yield behavior of reinforced concrete slab bridges. A detailed description of the methodology is given by Al-Sabah and Falter (2013) but is summarized below.

1.2.1 Rotation-Free Triangular Plate Element

A typical plate element has three degrees of freedom per node: one vertical displacement and two rotational. This element type needs to satisfy continuity of displacement and a first displacement derivative (slope) at its boundaries. Despite the considerable amount of research that has been devoted to plate elements, satisfying this type of continuity remains a challenge. One way of addressing this is to use a "rotation-free" plate element with fewer degrees of freedom (only one degree of freedom per node) along with a simpler formulation (Nay and

Utku 1972; Hampshire et al. 1992; Phaal and Calladine 1992). This element type is an evolution of the Morley's Triangle element concept (Morley 1971). The disadvantages of this element are the following: (i) the increased bandwidth in the global stiffness matrix due to the dependency of the element stiffness matrix on the surrounding elements, (ii) the sensitivity of rotation-free elements to mesh distortion, and (iii) the difficulty in defining rotational boundary conditions.

A rotation-free element is presumed to have a constant curvature that can be related to the out-of-plane displacement of the nodes of the particular element and its three adjacent elements. The main difference between triangular, rotation-free elements arises from different methods used to relate element curvature to nodal displacement. Sabourin and Brunet (2006) use the approach, in which the rigid body rotations of the main element edges are related to the out-of-plane nodal displacements. The element curvature is then calculated from the three edge curvatures that are in turn calculated from the edge rotation. Phaal and Calladine (1992) use 2D quadratic polynomials to interpolate between the six out-of-plane nodal displacements and those of the three surrounding elements, where constant curvatures are obtained as derivatives of the displacement polynomial. Oñate and Cervera (1993) integrate the curvature over the element area to calculate the average constant curvature of the element. Among different methods of curvature calculation, Sabourin and Brunet's (2006) provides features that are more desirable for yield line analysis. Their element is also known as the rotation-free "S3" element.

To allow internal yield lines to pass through the element, the relationship between bending and rigid rotation angle is revised, in the work done by Al-Sabah and Falter (2013). The particular nature of the S3 element allows the incorporation of plastic rotation at the boundaries with the rigid rotation angles. The effect of a yield line is a stiffness reduction which is transformed to each side of an element using transformation tensors (Al-Sabah and Falter 2013). For example in Figure 1, for the internal yield line inclined at an angle ϑ, relative to edge 2-3, the tangent stiffness parallel to the yield line (parallel to $\acute{x}$) is reduced to zero.
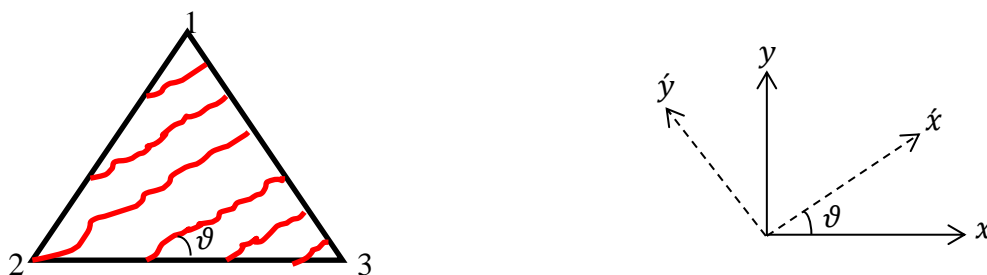

Figure 1 Yield-line coordinate system

In nonlinear analysis, load is applied in increments. When the material is idealized as elastic perfectly-plastic, the structure will exhibit multi-linear behavior, which can be used to simplify the nonlinear analysis by eliminating the iterations that usually follow each load

increment in order to satisfy equilibrium. In each load increment, the principal bending moment is compared to the bending moment capacity. Yield lines are created at elements with moment closest to yield and consequently the element stiffness is reduced to a small value parallel to the yield line direction. Using small, non-zero, values avoids introducing numerical instability.

The convergence criterion is based on the deflection-load ratio at a certain node. It is the ratio of two quantities; the incremental deflection ratio and the incremental load ratio. These two ratios are defined as the incremental to the total value for both deflection at a certain node and load. The solution stops when the deflection-load ratio exceeds a threshold which is set to 50 in this analysis.

1.3 Realistic Traffic Load Model

For a realistic site-specific load model, the simulation procedure developed by Enright (2010) and Enright and OBrien (2012) is used herein. They present a comprehensive model for the Monte Carlo simulation of free-flowing traffic on short to medium span bridges, for which the combined static and dynamic load effects produced by free-flowing traffic are taken to govern. In longer spans, static loading produced by congested traffic is generally considered to be more critical. In the model, the parameters for each individual truck and for the relative truck positions in each lane are simulated based on statistical distributions derived from the measured traffic at each site. For Gross Vehicle Weight (GVW) several models are proposed in the literature (Jacob 1991; Kennedy et al. 1992; Cooper 1995; Crespo-Minguillón and Casas 1997; Bailey and Bez 1999; O'Connor and OBrien 2005; OBrien et al. 2006). In this simulation, the GVW and number of axles for each truck is simulated using the 'semi-parametric' approach proposed by OBrien et al. (2010). Below a specified GVW threshold, an empirical (bootstrap) bivariate distribution is used to generate GVW and number of axles. Beyond this threshold, the tail of a bivariate Normal distribution is fitted to the frequencies to smooth the trend where data are sparse. The Normal distribution is chosen as it is widely used, is unbounded, and fits the data reasonably well.

For axle spacing, Enright (2010) describes the method adopted in this paper in which an empirical distribution is used to simulate the maximum axle spacing for each vehicle. For all other spacings, a trimodal Normal distribution is fitted to the data. Further details on the modeling of axle spacings are given elsewhere (Enright 2010; Enright and OBrien 2012).

For the weight of individual axles, many different approaches have been used in the literature (Harman and Davenport 1979; Grave et al. 2000; Miao and Chan 2002; OBrien et al. 2006). Enright (2010) uses bimodal Normal distributions for each axle in each vehicle class. The random variable used is the proportion of the GVW carried by each axle. In the measured data, the greatest variability is observed in the proportion of the GVW carried by each of the front four axles (Enright 2010).

To simulate headways (the time between the front axles of successive vehicles arriving at the same point on the road) a wide variety of distributions are proposed including the following: the negative exponential, uniform, gamma, and lognormal (OBrien and Caprani 2005). Here, the inter-axle gap (the gap between the rear axle of the leading truck and the front axle of the following truck) is used as an approximation for the clear gap between successive vehicles. A similar approach to that described by OBrien and Caprani (2005) is used herein to fit gap distributions to the observed data at different traffic flows. A negative exponential distribution is used for gaps greater than 4 seconds. To account for the observed correlation between gaps and the GVW of each truck (i.e. heavier trucks are likely to travel further apart), modifications are made to the gap distribution; successive gaps are not fully independent, as small gaps tend to occur in clusters (i.e. the gap behind a vehicle is dependent to some extent on the gap in front of it).

1.4 Nonlinear versus Linear Analyses

A 1000-year simulation was performed for site-specific extreme traffic load scenarios for two-lane opposing-direction traffic at three sites in the following countries: The Netherlands, Slovakia, and the Czech Republic. The characteristics of these sites are described by Enright (2010). The simulated traffic is run over three bridge lengths: 10 m, 15 m, and 20 m. For each length, 1000 maximum-per-year mid-span bending moments are calculated, along with details of the corresponding loading scenarios. For ease of computation, these annual maximum moments are based on a 1D linear elastic analysis of a simple beam, with no adjustment for transverse load distribution between lanes.

It should be noted that, due to the randomness inherent in the process, successive 1000-year simulation runs do not produce identical results, and the variation between runs becomes more pronounced in the upper tail. Running simulations for much longer periods – 10 000 years or more – is one way of reducing the variation at 1000 years, and indeed obviate the need to fit any distribution to the results. However it has been found that fitting a suitable distribution to the 1000-year simulation results allows characteristic load effects to be estimated accurately, with minimal bias and variation. In other words, good results are found when the length of the simulation equals or exceeds the specified return period.

Figure 2 shows the maximum mid-span moments for a simply supported bridge for the WIM data from the Czech Republic, plotted on Gumbel probability paper (Ang and Tang 2007). The Gumbel probability paper is created by linearization of cumulative probability function for extreme value distributions, where the y axis is double logarithm of cumulative probability distribution.

In all three cases, the trend is reasonably linear, thereby confirming good agreement with the Gumbel extreme value distribution. An upwardly curving trend in the graph would suggest that the solution is bounded, i.e., there is a physical upper limit to the load effect. The fact that this is not the case suggests that overload is being poorly controlled or that permits are being issued for vehicles that generate some very large load effects.

Unlike the conventional extrapolation approach, this long-run simulation retains information about what combinations of vehicles are critical for the most rare, extreme cases. This makes it possible, for the first time, to compare 1D analysis with 2D, and linear analysis with nonlinear, to determine if the ranking of the critical loading scenarios varies with the method of analysis. Due to the high computational cost of 2D nonlinear analysis, only the top 30 extreme scenarios are analyzed in this way, which is shown as the upper zone in Figure 2.

(a)

(b)
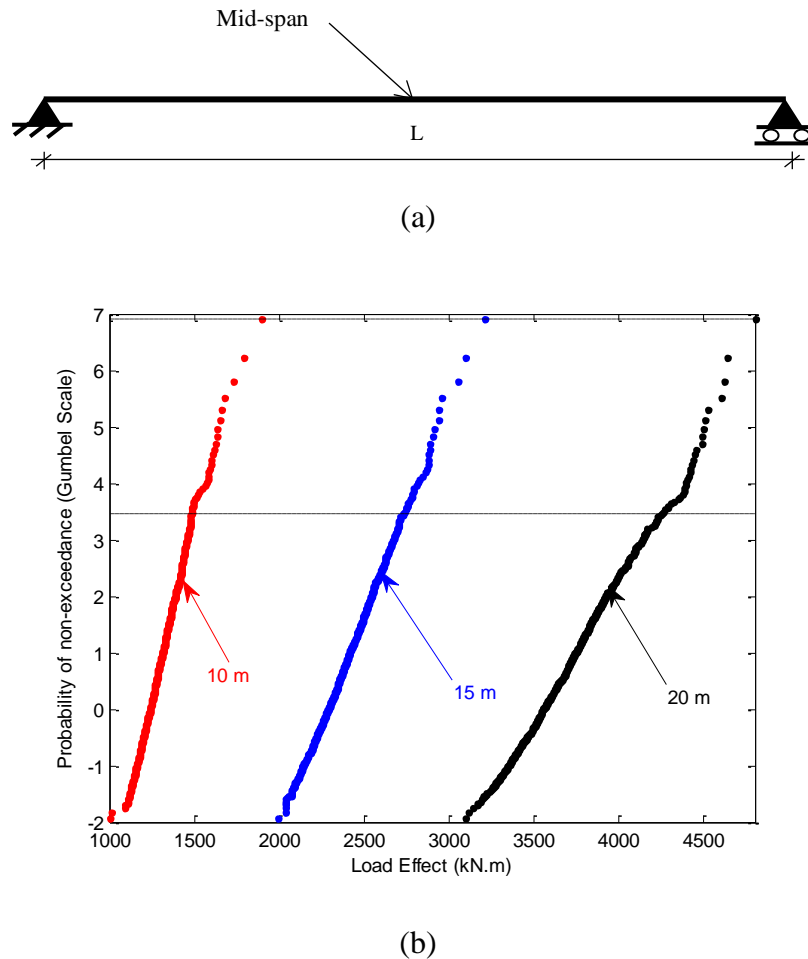
Figure 2 Annual maximum bending moments from 1000-year long-run simulations for Czech Republic: (a) bridge geometry; (b) probability paper plot

1.4.1 Detailed Analysis of an Extreme Scenario - Czech Republic

For the 20 m long bridge, the most critical load effect identified in the simulation based on the Czech WIM data is at the upper rightmost point in Figure 2. This scenario consists of a 5-axle and an 8-axle trucks moving in opposing directions. In this study, three types of analyses are used to calculate the load ratio for this particular scenario – 1D, 2D linear, and 2D nonlinear. For each analysis type, the vehicles are progressively moved over the bridge to find the most critical position. The load ratio is simply the ratio of bending moment capacity to maximum applied bending moment resulting from the load scenario. As the 1D beam is

determinate, the linear and nonlinear analyses give the same results (i.e., the 1D analysis is both linear and nonlinear).

The characteristic cylinder strength, f_{ck}, is selected to be 35 N/mm^2 with the reinforcement having a characteristic yield strength, f_{yk}, of 500 N/mm^2. The bridge deck is taken to be 10.5 m wide, and a span/depth ratio of 20 is used. The 1D characteristic bending moment capacity calculated according to EN 1992-2 for a 20 m bridge is 19 404 kNm. The characteristic bending moment capacity for a 10 m bridge is 4 483 kNm, and 9 523 kNm for a 15 m bridge.

For the 2D linear analysis, the slab illustrated in Figure 3 is modelled using a rectangular plate element with both bending and membrane capabilities (i.e., three degrees of freedom per node). Failure is defined by the element with the maximum moment. Figure 4 shows the load positions for the 1D (black arrows), 2D linear (blue outline and shaded) and 2D nonlinear analyses (red outline, not shaded) at failure.
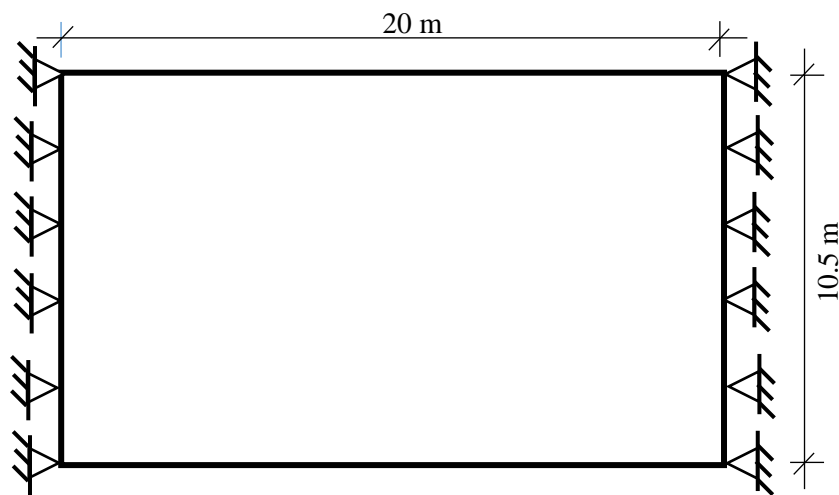

Figure 3 Plan view of slab bridge deck

For the 2D nonlinear analysis, the program developed by Al-Sabah and Falter (2013) is used. Figure 4(c) illustrates this case. It can be seen that the load position for the 2D nonlinear analysis is closer to the 1D linear critical load position than that for the 2D linear analysis (i.e., the solid red line (first axle of Truck1 in 2D nonlinear analysis) is closer to the black dashed line (first axle of Truck 1 in 1D analysis) than it is to the blue dotted line (first axle of Truck1 in 2D linear analysis)). These differences are relatively small (maximum difference is 0.84 m, which is 4% of the span).
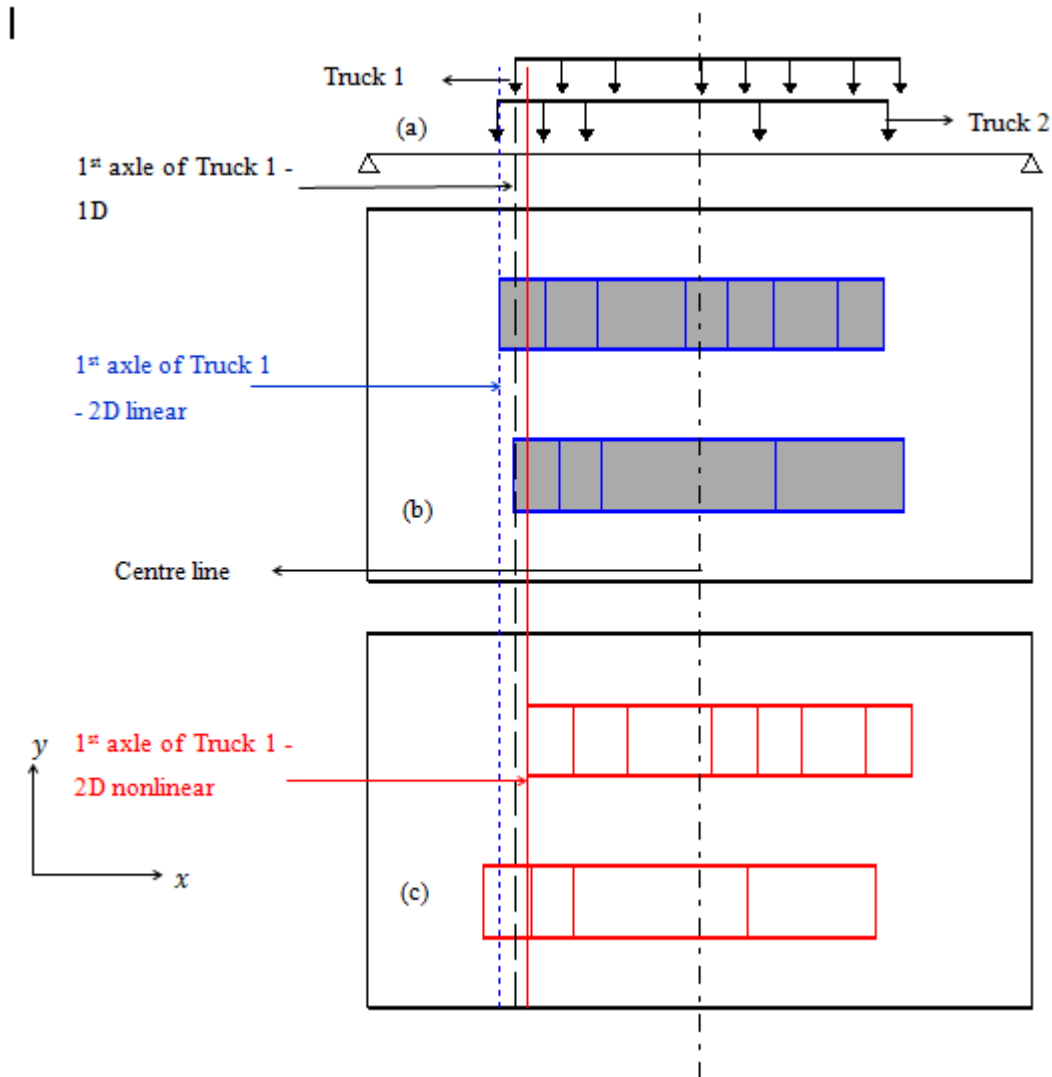
Figure 4 Axle position at critical case (minimum load ratio): (a) 1D linear analysis; (b) 2D linear analysis; (c) 2D nonlinear analysis – 20 m bridge, Czech Republic

Figure 5 shows the yield line pattern for the critical load position, just prior to failure. The yielding starts from the north edge, then develops at the south edge, and finally extends through the center of the slab. Higher elastic moments at the edges are explained in the contour plot of 2D linear elastic moments of Figure 6(a). These moments are higher at the north edge, because the 8-axle truck in the north lane is heavier than the truck in south lane. The bending moment contours for the 2D nonlinear analysis, as illustrated in Figure 6(b), show that the plastic yielding results in a more uniform moment distribution. The 'pixelated' pattern is due to the constant curvature assumption in the triangular rotation-free elements. This figure also confirms the yield pattern shown in Figure 5(b).
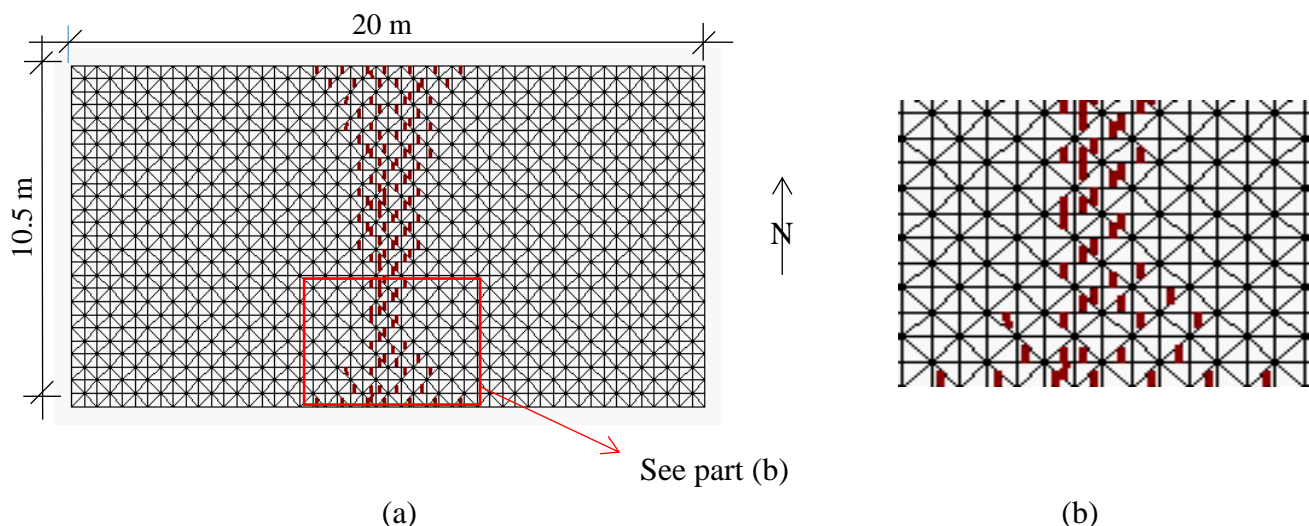
Figure 5 Yield line pattern for 2D nonlinear analysis: (a) Overview; (b) detail of yield line pattern at south edge
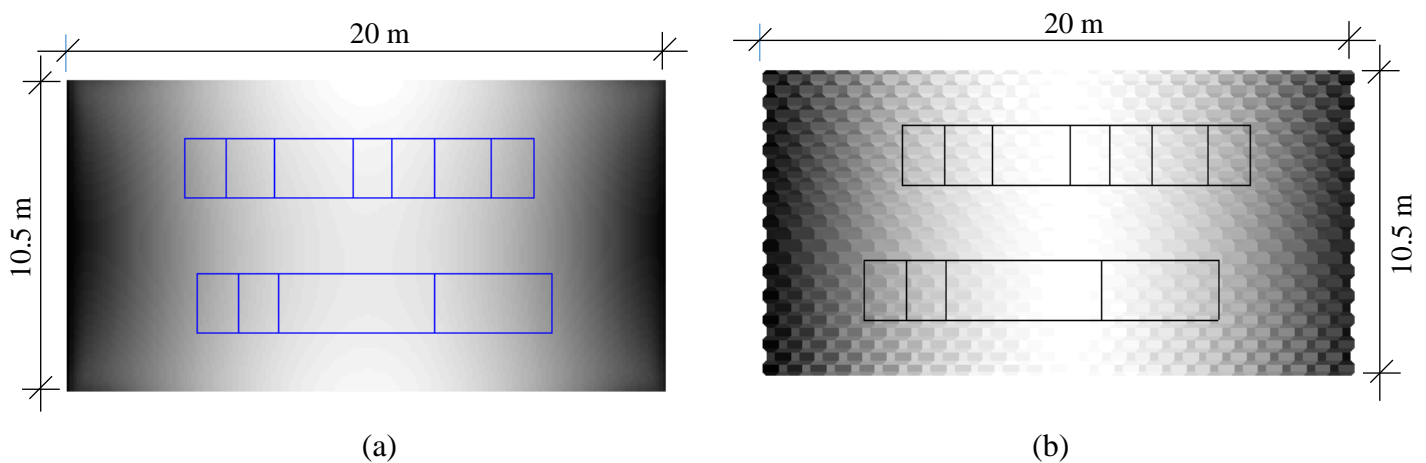

Figure 6 Bending moment contours for critical case (light color indicates higher moment): (a) 2D linear analysis; (b) 2D nonlinear analysis

1.4.2 Analysis of 30 Extreme Scenarios - Czech Republic

For the Czech WIM data, the 30 scenarios that give the greatest moments for the 1D analysis are considered further. These scenarios are shown by points over dashed line in Figure 2. First, load ratios are calculated for all 30 scenarios for each method of analysis (Figure 7). The scenarios are ranked according to the magnitude of the moment resulting from the 1D analysis. Figure 7(a) shows the load ratios versus scenario number. It shows that the 1D load ratios are in good agreement with the 2D nonlinear analysis. This can be explained by the fact that the yield pattern in the 2D analysis crosses the slab width, at which point it approaches the 1D case. The 1D failure corresponds, roughly speaking, to the point when the average 2D bending moment capacity is reached. The 2D linear analysis results in a much lower load effect, since it only considers the first yield situation. The load ratio generally increases with scenario number, which is not surprising, since the 30th scenario corresponds to the least critical scenario (i.e., lowest 1D bending moment at mid-span). Figure 7(b) shows the same load ratios against the bending moment at mid-span as calculated by the 1D linear analysis.

These bending moments are due to traffic loading and do not include bending moments resulting from self-weight. This plot also shows that the load ratio decreases with the increase in load effect (bending moment at mid-span). The 2D linear analysis does not show any particular trend, and this can be explained by the high sensitivity of first yield to local effects.
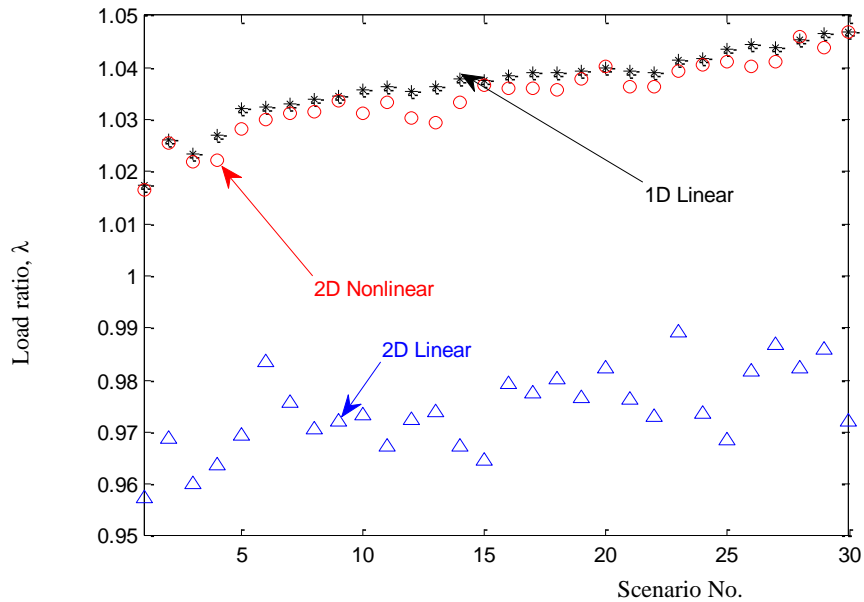
(a)
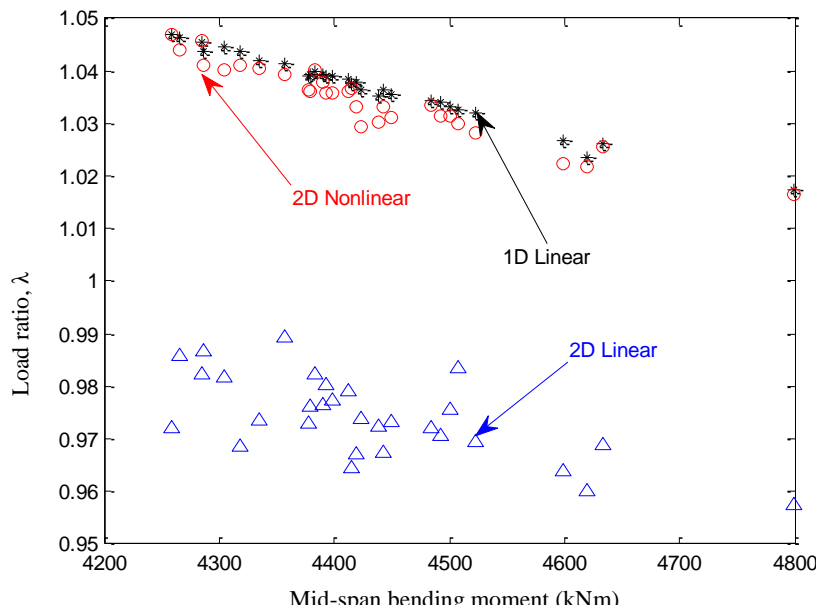
(b)

Figure 7 Load ratio for the 30 most critical loading scenarios for 20 m slab bridge in Czech Republic: (a) load ratio versus scenario number; (b) load ratio versus 1D bending moment at mid-span

These calculations are repeated for the 10 m and 15 m long bridges and all the results are presented in Figure 8. As can be seen in Figure 8, the slope of load ratio vs. load effect decreases with an increase in bridge length. Notably, the load ratio for the longer bridge resulting from a 2D linear analysis, is less scattered.
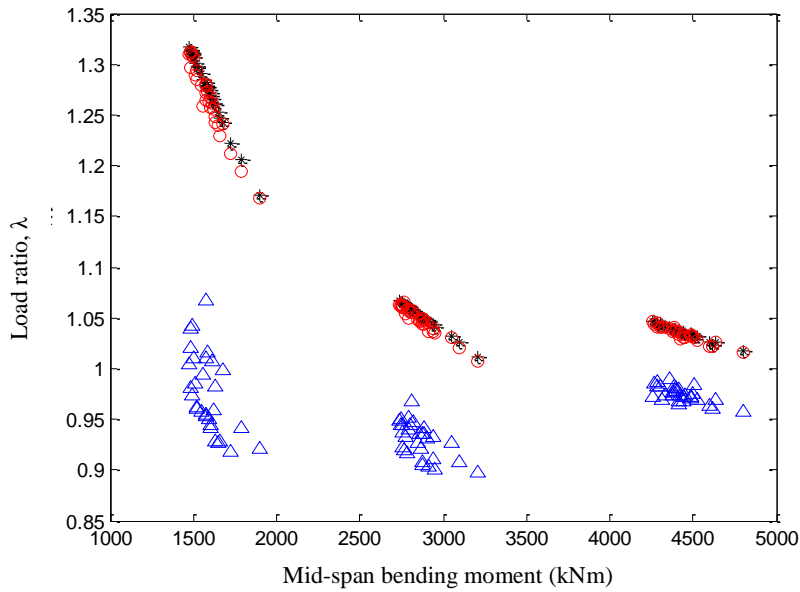
Figure 8 Load ratio for three types of analyses – Czech Republic

In Figure 9, the scenarios that are most critical for the 2D nonlinear analysis are compared to those that were most critical for the 1D analysis. The top 30 scenarios for a 20 m bridge in the Czech Republic site are considered for this purpose. It can be seen in the figure, for example, that the 2nd most critical scenario for the 1D analysis, is the 3rd ranked one in the 2D analysis. The greatest change in rank is from 6th (in 1D) to 13th (in 2D). Figure 9 shows that the top 10 ranked scenarios based on load ratios using 2D nonlinear analysis includes 8 from the top 10 scenarios ranked by the 1D linear mid-span bending moment.
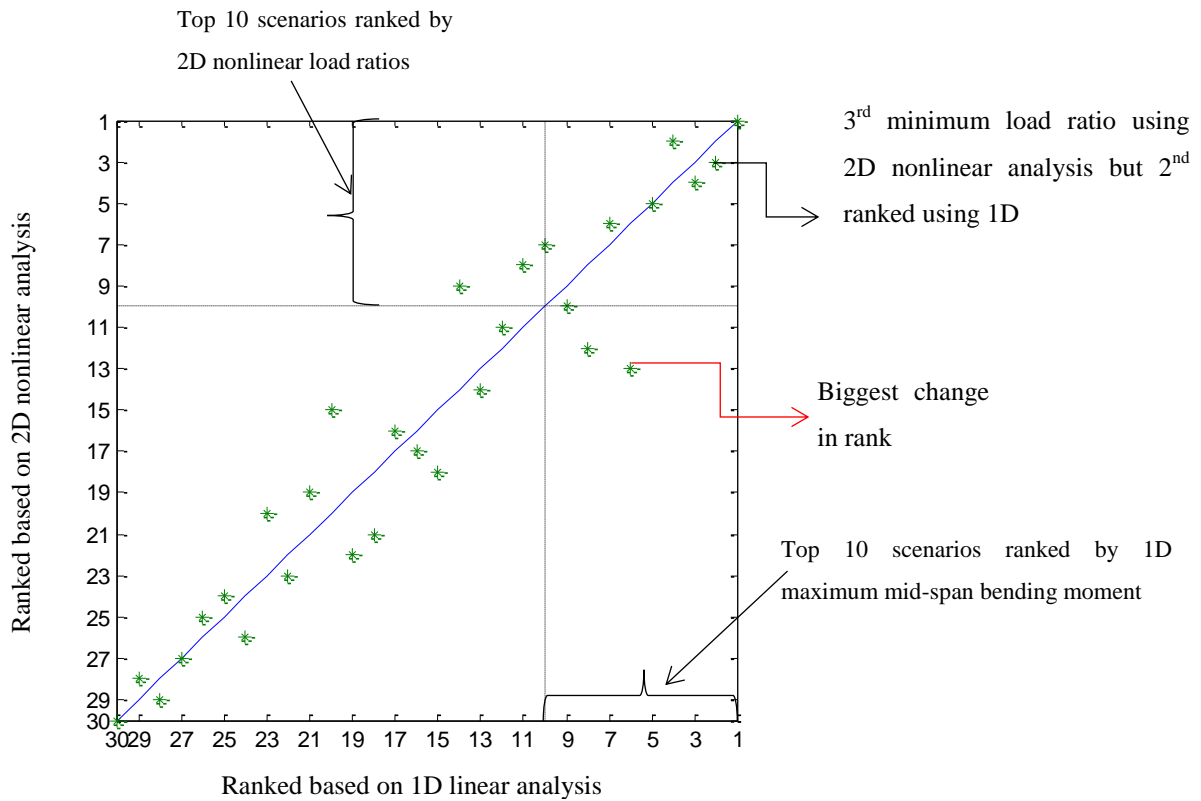

Figure 9 Loading scenario ranking based on ranked 1D linear mid-span bending moment and 2D nonlinear load ratio – Czech Republic

For the most extreme loading scenarios in each case, Figure 10 compares the bending moment distributions across the width of the slab. This figure shows the difference between the bending moment distributions at the critical position using the 2D and 1D linear analyses. The distribution for the 20 m bridge is flatter than the other two, which can be explained by two phenomena: (i) higher transverse load sharing in longer bridges, (ii) traffic scenarios with heavy vehicles in both lanes feature more frequently for longer bridges (i.e., shorter spans are more likely to be governed by single-truck events).
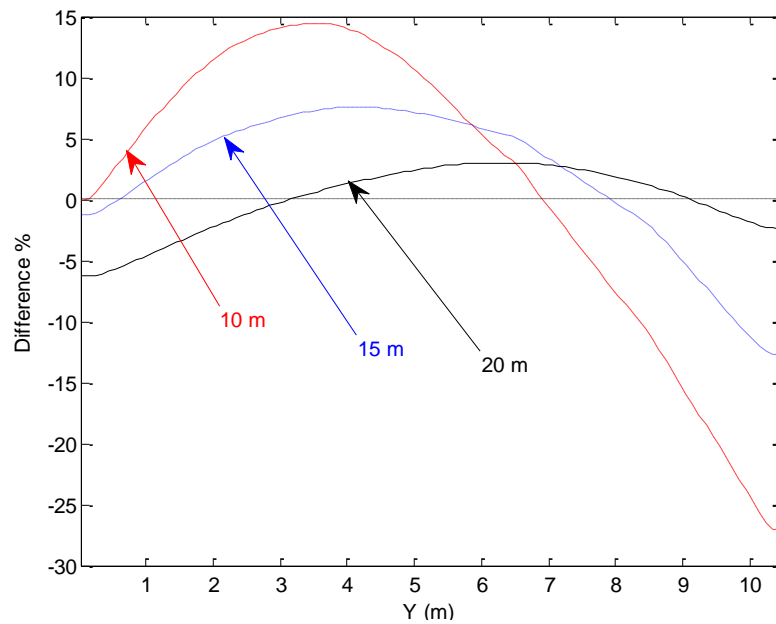

Figure 10 Difference in bending moment distribution between 2D and 1D linear analyses

Figure 11 gives the bending moment contours for the 2D linear analyses, confirming the results shown in Figure 10. In the 10 m slab, the load in lane 1 (south edge) is heavier than the load in lane 2 (north edge), which results in an asymmetrical distribution of bending moments across the bridge. The distribution becomes more symmetrical for longer spans because, for longer spans, there tends to be a greater degree of load sharing. This explains why the differences between 2D nonlinear and 2D linear analyses are greater for the shorter spans − see Figure 8. To further illustrate this phenomenon, the differences between the 2D linear and 2D nonlinear transverse distributions of bending moment are plotted in Figure 12 for the 30 most critical loading scenarios. It can be seen that the differences are less for greater spans (compare Figure 12(c) with Figure 12(a)).
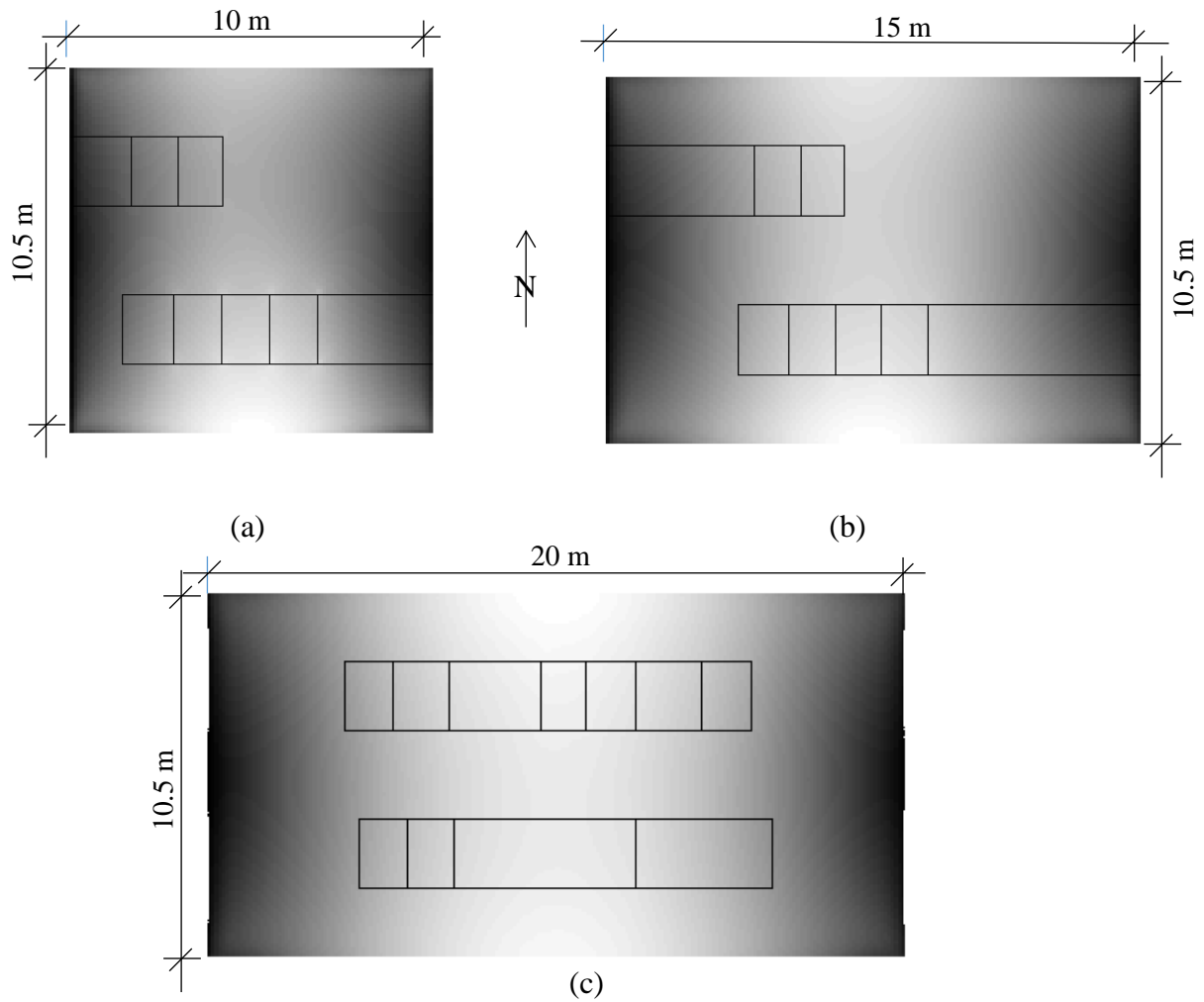
Figure 11 Bending moment contours at critical load position for an event with two trucks meeting (light color indicates higher moment): (a). 10 m, (b). 15 m and (c). 20 m bridge
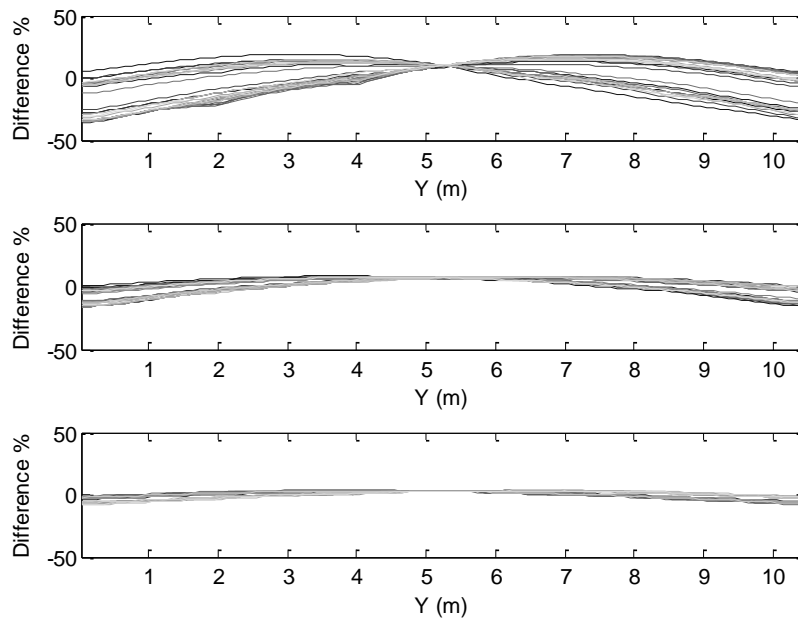

Figure 12 Differences in the top 30 bending moment distribution between 1D and 2D linear analyses across the slab width: (a) 10 m, (b) 15 m, and (c) 20 m bridge

1.4.3 Analysis of 30 Extreme Scenarios - Three Different Sites

The same procedure is applied to calculate the load ratio for the WIM sites in the Netherlands and Slovakia. Figure 13 uses Gumbel probability paper to show the bending moment at mid-span using 1D analysis for all sites and bridge lengths. Traffic in the Netherlands has a much higher proportion of very heavy vehicles (e.g., 0.03% of vehicles in excess of 100 t compared with only 0.002% in the Czech Republic), which results in considerably higher bending moments at mid-span. In comparison, both the Czech Republic and Slovakia have considerably lower bending moments with the former being a little higher than the latter.
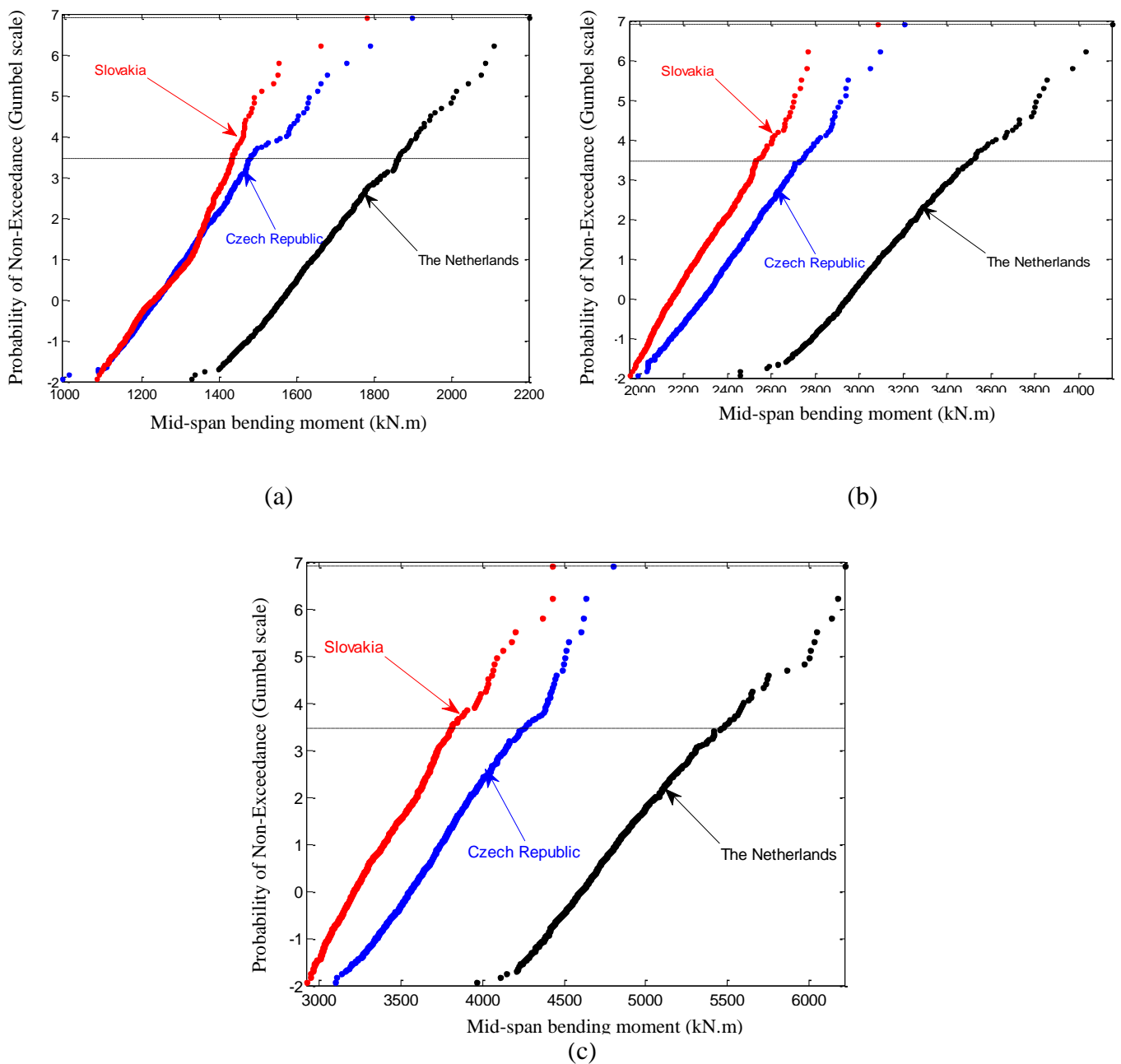

(a)
(b)

(c)

Figure 13 Annual maximum bending moment distribution for different sites: (a) 10 m; (b) 15 m; (c) 20 m bridge

One of the findings from Enright's work (Enright 2010) is that, as the GVW increases to extremely high values, low loaders and crane-type vehicles become the predominant vehicle types. Detailed analysis of the three examined data sets shows: WIM data from the Netherlands includes 2.4% crane-type and 3.8% low loaders compared to Slovakia with 1.7% crane-type and 1.0% low loaders and the Czech Republic with 0.7% cranes and 3.4% low loaders. This is a reflection of the much higher proportion of extremely heavy vehicles at the site in the Netherlands.

Figure 14 shows the load ratio for the 1D analysis for the three sites and three lengths. Load effects calculated using Czech and Slovakian data overlap but there is a clear gap between these and the load effects corresponding to the much heavier vehicles found in the Dutch data.
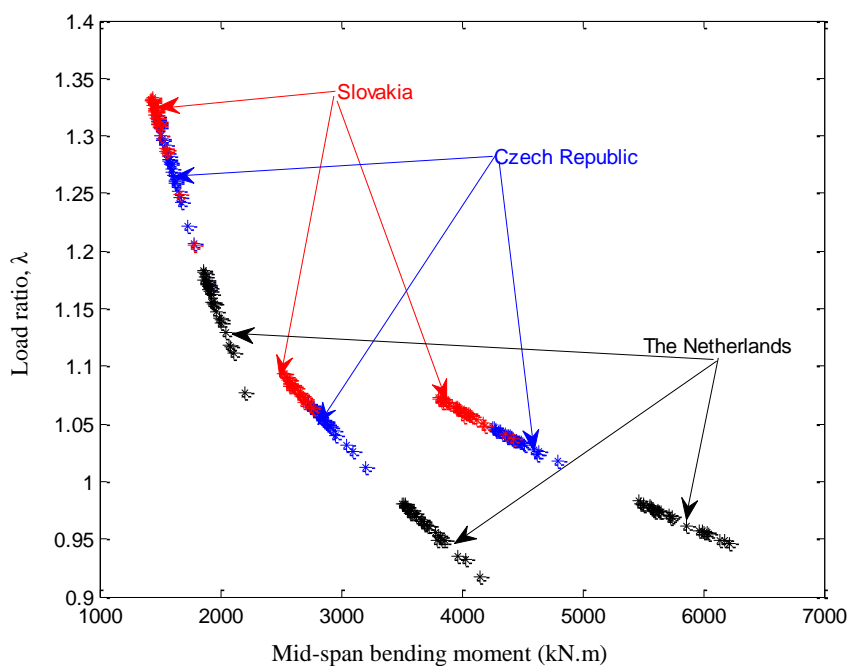

Figure 14 Load ratio based on 1D analysis for different sites and different total lengths

The results of the 2D nonlinear analysis results are very similar, as illustrated in Figure 15(a). However, as seen in other figures, the relationship between load ratio and bending moment is much more variable in the 2D linear analysis results of Figure 15(b).

Given the high cost of computation needed for 2D nonlinear analysis, it can be concluded that the 1D linear analysis is a good alternative to obtain an estimation of the load ratio for a simply supported isotropic bridge slab, subjected to extreme traffic loads. In contrast, the 2D linear analysis is quite conservative for load ratio calculation for this type of bridge if sufficient ductility exists to allow the yield lines to form.
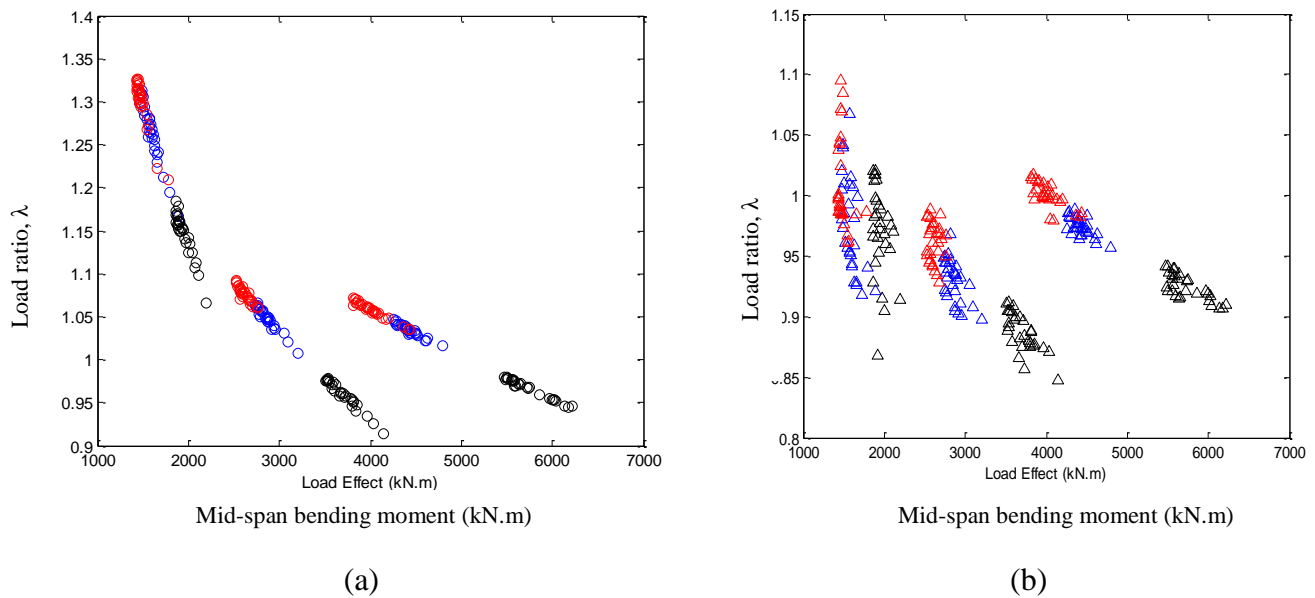
Figure 15 Load ratio for different sites and different total lengths: (a) 2D nonlinear; (b) 2D linear

Comparing the critical scenarios in the 1D analyses to those that are most critical for the 2D nonlinear analyses reveals a high degree of similarity. For the Dutch site, the top 10 ranked scenarios for the 1D analysis include all of the top 10 ranked for 2D nonlinear analysis. This is true for all three spans at this site. In Slovakia, this type of comparison shows that, for total lengths of 10 m and 15 m, 8 of 10 ranked scenarios for 1D mid-span bending moments are also in the 2D nonlinear top 10. For the 20 m bridge, 9 of the top 10 1D are in the 2D nonlinear top 10. The 1D and 2D nonlinear rankings for the Czech data give results similar to those for Slovakia.

1.5 Conclusion

Extreme traffic loading is investigated for a range of single-span isotropic slab bridges using weigh-in-motion data from three different European sites. Long-run simulations make it possible to identify the combinations of vehicles that govern near the maximum-in-1000-year level. The 30 most critical loading scenarios in the 1D analyses are used in 2D linear and nonlinear analyses. It is found that the ranks do not change significantly, i.e., the most critical scenarios from the 1D linear/nonlinear analyses are also the most critical in 2D linear and 2D nonlinear analyses. There are small differences in the precise locations of the vehicles that govern.

As the bridges are all isotropic, the 2D nonlinear yield line runs straight across near the center in all cases. This is very similar to the result that is found from a 1D analysis where linear and nonlinear are the same. A 2D linear analysis is more conservative – first yield occurs at a significantly lower level of load than that required to cause plastic collapse. The difference between the 2D linear and 2D nonlinear analyses is less for longer spans as there is a greater degree of load sharing so the transverse variation in elastic moment is less.

References

Al-Sabah, A. S., & Falter, H. (2013). Finite Element Lower Bound "Yield Line" Analysis of Isotropic Slabs Using Rotation-Free Elements. *Engineering Structures, 53*, 38-51.

Ang, A. H.-S., & Tang, W. H. (2007). *Probability Concepts in Engineering Planning and Design - Basic Principles* (2 ed.). Unites States of America: John Wiley & Sons.

Bailey, S. F., & Bez, R. (1999). Site Specific Probability Distribution of Extreme Traffic Action Effects. *Probabilistic Engineering Mechanics, 14*(1), 19-26.

Bauer, D., & Redwood, R. G. (1987). Numerical Yield Line Analysis. *Computers and Structures, 26*(4), 587-596.

Burgoyne, C. J., & Smith, A. L. (2008). Automated Lower Bound Analysis of Concrete Slabs. *Magazine of Concrete Research, 60*(8), 609-622.

Cooper, D. I. (1995). The Determination of Highway Bridge Design Loading in the United Kingdom from Traffic Measurements. *First European Conference on Weigh-In-Motion of Road Vehicles*, Zurich, Switzerland. 413-421.

Crespo-Minguillón, C., & Casas, J. R. (1997). A Comprehensive Traffic Load Model for Bridge Safety Checking. *Structural Safety, 19*(4), 339-359.

Dawe, P. (2003). *Research Perspectives: Traffic Loading on Highway Bridges*. London, United Kingdom: Thomas Telford.

Dickens, J. G., & Jones, L. L. (1988). A General Computer Program for the Yield-Line Solution of Edge Supported Slabs. *Computers and Structures, 30*(3), 465-476.

Enright, B. (2010). *Simulation of Traffic Loading on Highway Bridges.* PhD Thesis, University College Dublin, Dublin, Ireland.

Enright, B., & OBrien, E. J. (2012). Monte Carlo Simulation of Extreme Traffic Loading on Short and Medium Span Bridges. *Structure and Infrastructure Engineering, 9*(12), 1267-1282.

Gindy, M., & Nassif, H. H. (2006). Comparison of Traffic Load Models Based on Simulation and Measured Data. *Joint International Conference on Computing and Decision Making in Civil and Building Engineering*, Montreal, Canada. 2497-2506.

Gohnert, M. (2000). Collapse Load Analysis of Yield-Line Elements. *Engineering Structures, 22*(8), 1048-1054.

Gohnert, M., & Kemp, A. R. (1995). Yield-Line Elements: for Elastic Bending of Plates and Slabs. *Engineering Structures, 17*(2), 87-94.

Grave, S. A. J., OBrien, E. J., & O'Connor, A. J. (2000). The Determination of Site-Specific Imposed Traffic Loadings on Existing Bridges. *The Fourth International Conference on Bridge Management*, Surrey. 442-449.

Hajializadeh, D., OBrien, E. J., Enright, B., & Sheils, E. (2012). Nonlinear Response of Structures to Characteristic Loading Scenarios. *Joint Conference of the Engineering Mechanics Institute and 11th ASCE Joint Specialty Conference on Probabilistic Mechanics and Structural Reliability, EMI/PMC 2012*, Notre Dame, IN, United States of America.

Hampshire, J. K., Topping, B. H. V., & Chan, H. C. (1992). Three Node Triangular Bending Elements with One Degree of Freedom per Node. *Engineering Computations, 9*(1), 49-62.

Harman, D. J., & Davenport, A. G. (1979). A Statistical Approach to Traffic Loads on Highway Bridges. *Canadian Journal of Civil Engineering, 6*(4), 494-513.

Hillerborg, A. (1975). *Strip Method of Design*. California, United States of America: Cement and Concrete Association.

Ingerslev, A. (1923). Strength of Rectangular Plates. *Journal of Structural Engineering, 1*, 3-14.

Jackson, A. M., & Middleton, C. R. (2009). Generalised Method for Predicting the Flexural Collapse Load of Concrete Slabs. *Proceedings of the Annual International fib Symposium Concrete: 21st Centruy Superhero, Building a Sustainable Future*, London, United Kingdom.

Jacob, B. (1991). Methods for the Prediction of Extreme Vehicular Loads and Load Effects on Bridges *Report of Subgroup 8, Eurocode 1. Traffic Loads on Bridges* Paris, France: Laboratoire Central des Ponts et Chaussées, LCPC.

Jennings, A., Thavalingam, A., McKeown, J. J., & Sloan, D. (1993). On the Optimisation of Yield Line Patterns. In B. H. V. Topping (Ed.), *Developments in Computations Engineering Mechanics, Civil-Comp Press, Edinburgh* (pp. 209-214).

Johansen, K. W. (1962). *Yield-Line Theory*. London, United Kingdom: Cement and Concrete Association.

Johnson, D. (1994). Mechanism Determination by Automated Yield-Line Analysis. *The Structural Engineer, 72*(19), 323-327.

Johnson, D. (1995). Yield-Line Analysis by Sequential Linear Programming. *International Journal of Solids and Structures, 32*(10), 1395-1404.

Johnson, D. (1996). Automated Yield-Line Analysis of Orthotropic Slabs. *International Journal of Solids and Structures, 33*(1), 1-10.

Jones, L. L., & Wood, R. H. (1967). *Yield-Line Analysis of Slabs*. London, United Kingdom: Thames & Hudson.

Kennedy, D. J. L., Gagnon, D. P., Allen, D. E., & MacGregor, J. G. (1992). Canadian Highway Bridge Evaluation: Load and Resistance Factors. *Canadian Journal of Civil Engineering, 19*(6), 992-1006.

Kwan, A. K. H. (2004). Dip and Strike Angles Method for Yield Line Analysis of Reinforced Concrete Slabs. *Magazine of Concrete Research, 56*(8), 487-498.

Miao, T. J., & Chan, T. H. T. (2002). Bridge Live Load Models from WIM Data. *Engineering Structures, 24*(8), 1071-1084.

Morley, L. S. D. (1971). The Constant-Moment Plate-Bending Element. *The Journal of Strain Analysis for Engineering Design, 6*(1), 20-24.

Munro, J., & Da Fonseca, A. M. A. (1978). Yield Line Method by Finite Elements and Linear Programming. *The Structural Engineer, 56B*(2), 37-44.

Nay, R. A., & Utku, S. (1972). An Alternative to the Finite Element Method. *Variational Methods in Engineering*, Southampton, United Kingdom. 62-74.

Nielsen, M. P. (1964). Limit Analysis of Reinforced Concrete Slabs *Acta Polytechnica Scandinavica, Civil Engineering and Building Construction Series* (Vol. 26). Danmark: København.

Nowak, A. S. (1993). Live Load Model for Highway Bridges. *Structural Safety,* **13**(1-2), 53-66.

O'Dwyer, D. W., & OBrien, E. J. (1998). Design and Analysis of Concrete Slabs Using a Modified Strip Method. *The Structural Engineer,* **76**(17), 329-333.

O'Connor, A. J., & Enevoldsen, I. (2009). Probability-Based Assessment of Highway Bridges According to the New Danish Guideline. *Structure and Infrastructure Engineering,* **5**(2), 157-168.

O'Connor, A. J., & OBrien, E. J. (2005). Traffic Load Modelling and Factors Influencing the Accuracy of Predicted Extremes. *Canadian Journal of Civil Engineering,* **32**(1), 270-278.

OBrien, E. J., & Caprani, C. C. (2005). Headway Modelling for Traffic Load Assessment of Short to Medium Span Bridges. *The Structural Engineering,* **83**(16), 33-36.

OBrien, E. J., Caprani, C. C., & O'Connor, A. J. (2006). Bridge Assessment Loading: a Comparison of West and Central/East Europe. *Bridge Structures-Assessment, Design & Construction,* **2**(1), 25-33.

OBrien, E. J., Enright, B., & Getachew, A. (2010). Importance of the Tail in Truck Weight Modeling for Bridge Assessment. *Journal of Bridge Engineering,* **15**, 210-213.

Oñate, E., & Cervera, M. (1993). Derivation of Thin Plate Bending Elements with one Degree of Freedom per Node: a Simple Three Node Triangle. *Engineering Computations,* **10**(6), 543-561.

Phaal, R., & Calladine, C. R. (1992). A Simple Class of Finite Elements for Plate and Shell Problems. I: Elements for Beams and Thin Flat Plates. *International Journal for Numerical Methods in Engineering,* **35**(5), 955-977.

Sabourin, F., & Brunet, M. (2006). Detailed Formulation of the Rotation-Free Triangular Element "S3" for General Purpose Shell Analysis. *Engineering Computations,* **23**(5), 469-502.

Thavalingam, A., Jennings, A., McKeown, J. J., & Sloan, D. (1998). A Computerised Method for Rigid-Plastic Yield-Line Analysis of Slabs. *Computers and Structures,* **68**(6), 601-612.

Wüst, J., & Wagner, W. (2008). Systematic Prediction of Yield-Line Configurations for Arbitrary Polygonal Plates. *Engineering Structures,* **30**(7), 2081-2093.